Received: 18 November 2020 | Revised: 1 February 2021 | Accepted: 3 February 2021

DOI: 10.1002/nano.202000246

RESEARCH ARTICLE

Nano Select WILEY

Superwettability-based separation: From oil/water separation to polymer/water separation and bubble/water separation

Jiale Yong[1] | **Qing Yang**[2] | **Jinglan Huo**[1] | **Xun Hou**[1] | **Feng Chen**[1]

[1] State Key Laboratory for Manufacturing System Engineering and Shaanxi Key Laboratory of Photonics Technology for Information, School of Electronic Science and Engineering, Xi'an Jiaotong University, Xi'an, PR China

[2] School of Mechanical Engineering, Xi'an Jiaotong University, Xi'an, PR China

Correspondence
Feng Chen, State Key Laboratory for Manufacturing System Engineering and Shaanxi Key Laboratory of Photonics Technology for Information, School of Electronic Science and Engineering, Xi'an Jiaotong University, Xi'an, 710049, PR China.
Email: chenfeng@mail.xjtu.edu.cn

Funding information
National Key Research and Development Program of China, Grant/Award Number: 2017YFB1104700; National Science Foundation of China, Grant/Award Numbers: 61805192, 61875158; International Joint Research Laboratory for Micro/Nano Manufacturing and Measurement Technologies; Fundamental Research Funds for the Central Universities

Abstract

The separation of oil/water mixtures, polymer/water mixtures, or bubble/water mixtures has broad applications. In this paper, we aim at extending the well-developed wettability-based oil/water separation strategy to separate the mixtures of liquid polymers and water and separate bubbles from water. The micro/nanostructures are simply produced on a stainless steel mesh by femtosecond laser treatment to endow the mesh with superhydrophilicity in the air and superoleophobicity, superpolymphobicity, and superaerophobicity in water. The underwater superoleophobicity, superpolymphobicity, and superaerophobicity enable the structured mesh to have the ability of oil/water separation, polymer/water separation, and bubble/water separation. Water can pass through the mesh due to the superhydrophilicity of the laser-structured mesh. Whereas, the oils, the liquid polymers, and the bubbles in water are intercepted by the structured mesh because such a water-wetted mesh has strong repellence to oils (underwater superoleophobicity), liquid polymers (underwater superpolymphobicity), and bubbles (underwater superaerophobicity). As a result, the oil, the liquid polymer, and the bubble are successfully separated from water by using the as-prepared superwetting mesh. We believe that the diversified wettability-based separation processes will have wide potential applications in environmental protection, energy utilization, industrial manufacture, agricultural production, and so on.

KEYWORDS
bubble/water separation, oil/water separation, polymer/water separation, underwater superaerophobicity, underwater superpolymphobicity

1 | INTRODUCTION

The separation of different materials (such as liquid-liquid mixtures, liquid-gas mixtures) has significant value in both fundamental research and practical application.[1–7] Many novel materials and strategies have been developed to achieve such a function.[8–10] In the past decades, superwettability has been successfully applied in oil/water separation.[11–15] Based on the different wetting behaviors of oils and water, the mixture of oils and water can be

effectively separated by the porous materials with either superhydrophobicity or underwater superoleophobicity.[16–20] Feng et al. used a superhydrophobic and superoleophilic mesh to separate the mixture of water and oil.[21] Water was repelled by the mesh and thus maintained above the mesh, while oil wetted the mesh and passed through the mesh. Xue et al. further developed a method to separate oil/water mixtures by using a superhydrophilic and underwater superoleophobic mesh which allowed water to pass through but intercepted oils.[22] In fact, the mixtures that need to be separated are much more than a simple mixture of oil and water. Liquid polymers in water and underwater bubbles are also intractable problems.[23–29] Recently, superwetting states related to underwater polymers and bubbles are also developed, for example, underwater superpolymphobicity[23–25] and underwater superaerophobicity.[26–29] Similar to the oil repellence of the underwater superoleophobic surfaces, the underwater superpolymphobic materials greatly repel liquid polymers and the underwater superaerophobic materials repel bubbles in a water medium. Corresponding to the sole great success of superwetting materials in oil/water separation,[11–15] so far, an issue has been lingering in our mind: can the superwettability be also used to separate liquid polymers and tiny bubbles from water? The generalization of the wettability-based separation process from oil/water mixtures to other mixtures composed of different phases/materials remains a great challenge.

The aim of this paper is to enlarge the scope of the application of the wettability-based separation method. Here, we extend the method of oil/water separation to separate the mixtures of liquid polymers and water and the mixtures of bubbles and water based on the special surface wettability of the separation materials. Micro/nanostructures are simply produced on the wire surface of a stainless steel mesh by femtosecond laser treatment. The formation of micro/nanostructures makes the laser-treated mesh become superhydrophilic in air, while the structured mesh shows superoleophobicity, superpolymphobicity, and superaerophobicity in a water medium. By taking the advantages of the different wetting behaviors of the mesh to oil/polymer/bubbles and water, the oils, liquid polymers, and bubbles are successfully separated from water by using the as-prepared underwater superoleophobic, superpolymphobic, and superaerophobic mesh.

2 | RESULTS AND DISSCUSSION

2.1 | Surface microstructure and wettability

Usually, an extreme wetting state can be obtained by combining proper rough microstructure and chemistry.[30–34]

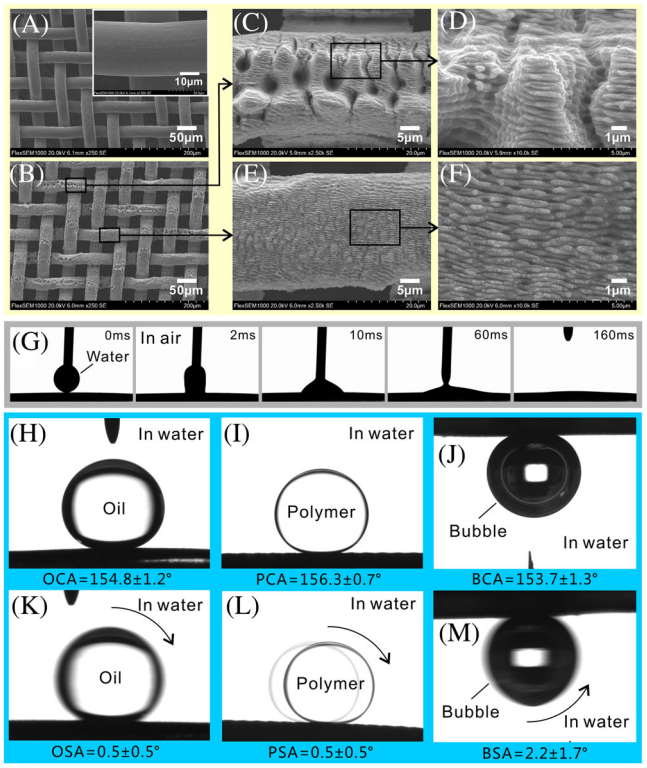

FIGURE 1 Surface microstructure and wettability of the femtosecond laser-structured stainless steel mesh. A, SEM images of an untreated mesh. The inset shows the SEM image at high magnification. B, SEM image of the mesh processed by a femtosecond laser. (C-F) Two kinds of laser-induced microstructures on the wire surface of the structured mesh: (C and D) the separated conical-shaped spikes and (E and F) the typical laser-induced periodic nanoripples. G, Process of a water droplet wetting the structured mesh. Static shapes of (H) an oil droplet, (I) a liquid polymer droplet, and (J) a bubble on the laser-ablated mesh underwater. (K) Oil droplet, (L) liquid polymer droplet, and (M) bubble rolling off on the laser-ablated mesh in water

For example, underwater superoleophobicity,[35–37] superpolymphobicity,[23–25] and superaerophobicity[26–29] can be achieved on a hydrophilic substrate by the formation of micro/nanoscale surface structures. The underwater superoleophobic microstructures greatly repel oils, the underwater superpolymphobic microstructures repel liquid polymers, and the underwater superaerophobic microstructures repel bubbles in a water medium.

The untreated stainless steel mesh has a smooth wire surface (Figure 1A). To obtain superwettabilities, a femtosecond laser is used to produce microstructures on the stainless steel mesh. The wire surface is roughed and composed of two kinds of microstructures after femtosecond laser treatment (Figure 1B). One is the separated conical-shaped spikes, as shown in Figure 1C and D. The spikes have a base diameter of ~3.2–9.6 μm and their surfaces are covered with the typical laser-induced nanoripples. Besides, many deep microholes form between

the microspikes. The microspikes are induced by the spot center of the focused laser beam.[23,38] Generally, the strongest ablation occurs at the focused point because of the highest laser fluence of the spot center. At the focused point, the metal substrate melts after absorbing the energy of the repetitious impulses and the melted metal explodes as the plasma expands and bursts out of the focal volume.[23,38] After the melted metal and the ejected metal cooling down and re-solidifying rapidly, separated microspikes and microholes appear at the spot center. On the other hand, some regions of the ablated mesh are only coated by nanoripples structure, as shown in Figure 1E,F. The period of the ripples is ~500–550 nm. The nanoripples are induced by the low-fluence spot fringe of the focused laser beam.[23,38]

The untreated stainless mesh shows a contact angle (CA) of 115.9° ± 6.1° to a water droplet due to the existence of the porous mesh microstructure, although stainless steel is a typical hydrophilic material. By contrast, a small water droplet can fully wet the structured mesh as the droplet is dripped onto the mesh (Figure 1G and Movie S1 in the Supporting Information). The water CA (WCA) of the droplet closes to 0°, indicating that the mesh becomes superhydrophilic after laser processing. Underwater wettability (including CA and sliding angle (SA)) is investigated after immersing the structured mesh in water. An underwater oil droplet has a spherical shape on the structured mesh, with an oil CA (OCA) of 154.8° ± 1.2° (Figure 1H). The oil SA (OSA) is as low as 0.5° ± 0.5° (Figure 1K and Movie S2 in the Supporting Information). Therefore, the generation of the laser-induced microstructures enables the stainless steel mesh to exhibit superoleophobicity and very low adhesion to oils in water; that is, the structured mesh is underwater superoleophobic and repels oils. Some polymers are also liquid state. Usually, liquid polymers have a more complex composition, higher viscosity, and lower fluidity compared to pure water and oils. Similar to oil droplets, the structured mesh also shows strong repellence to liquid polymers in a water medium. An underwater polymer droplet has a polymer CA (PCA) of 156.3° ± 0.7° on the structured mesh (Figure 1I). Once the mesh is slightly tilted, the polymer droplet will roll away, with a polymer SA (PSA) of 0.5° ± 0.5° (Figure 1L and Movie S2 in the Supporting Information). So, the structured mesh exhibits underwater superpolymphobicity. Underwater bubbles can also be repelled by the structured mesh. Small bubbles on the structured mesh have a bubble CA (BCA) of 153.7° ± 1.3° (Figure 1J) and a bubble SA (BSA) of 2.2° ± 1.7° (Figure 1 M and Movie S2 in the Supporting Information) in water, demonstrating the underwater superaerophobicity of the structured mesh. The bubble can keep a ball shape and easily roll off on the mesh. Therefore, the laser-induced microstructures endow the stainless steel mesh with superhydrophilicity, underwater superoleophobicity, underwater superpolymphobicity, and underwater superaerophobicity. The structured mesh shows remarkable repellence to oils, liquid polymers, and bubbles in the water.

The laser-induced microstructure plays an important role in the achievement of underwater superoleophobicity, superpolymphobicity, and superaerophobicity. Stainless steel is an inherently hydrophilic substrate. Usually, the rough surface microstructure can enhance the natural wettability of a solid material.[23–37] After the formation of conical-shaped spikes and nanoripples structure on the mesh surface by femtosecond laser treatment, the hydrophilicity of stainless steel is greatly amplified, because laser-induced rough microstructures can greatly increase the real surface area of the mesh substrate.[35] That is, rough microstructure makes hydrophilic substrate become more hydrophilic. As a result, the extreme state of hydrophilicity (i.e., superhydrophilicity) is exhibited by the structured stainless steel mesh. The contact between water and the mesh is at the Wenzel wetting state.[35,39,40] Water can entirely wet the laser-structured superhydrophilic mesh, as shown in Figure 2A. As the mesh is immersed in water, the holes of the mesh and the microstructures on the wire surface are completely wetted by water because of the superhydrophilicity. A layer of water is trapped by the superhydrophilic microstructures, which can provide a repulsive force to oils due to the repulsive interaction between water (polar) and oil (nonpolar) molecules. When an oil droplet is dripped onto the structured mesh in water, it is just allowed to sit on the top portion of the surface microstructures of the mesh due to the existence of the trapped water cushion. The oil droplet is at the underwater version of Cassie wetting state (Figure 2B).[35,39,40] The contact area between the oil and the mesh is effectively reduced by the laser-induced microstructures so that the mesh shows great repellence to oils in water (i.e., ultralow-adhesive underwater superoleophobicity). The achievement of underwater superpolymphobicity is similar to that of underwater superoleophobicity. When a liquid polymer droplet comes in contact with the structured mesh underwater, a water cushion forms underneath the polymer droplet, which greatly prevents the liquid polymer from touching the structured mesh due to the mutual exclusion and insolubility between water and polymer. The liquid polymer is also at the Cassie state on the structured mesh in water (Figure 2C). As a result, the structured mesh greatly repels polymers and exhibits superpolymphobicity in water. Regarding the underwater bubble on such superhydrophilic mesh, the inherent repellence between water and gas enables the trapped water cushion to prevent the bubbles from contacting the mesh.

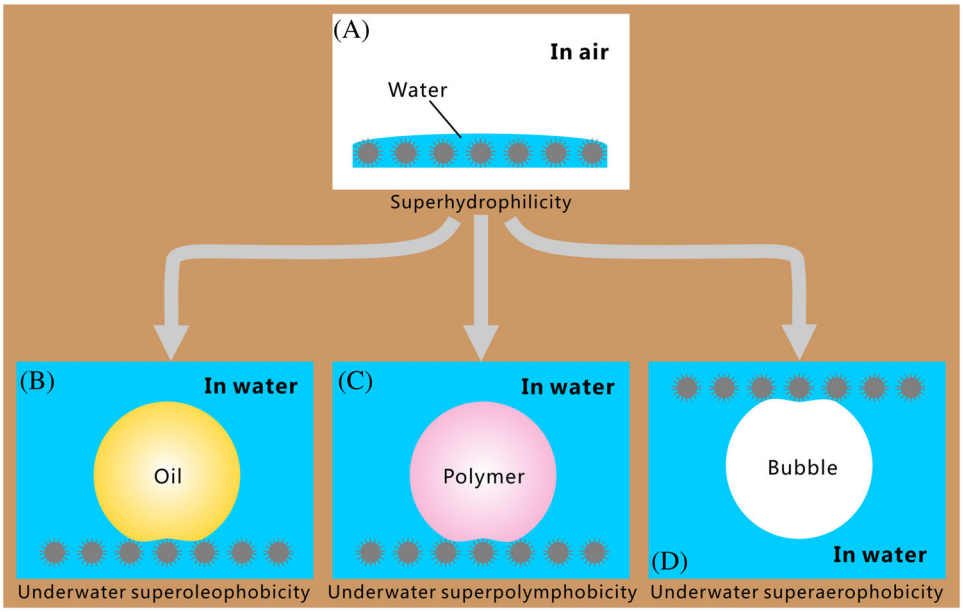

FIGURE 2 Formation mechanism of different underwater superwettabilities: from superhydrophilicity to underwater superoleophobicity, superpolymphobicity, and superaerophobicity. A, Schematic diagram of a water droplet on the laser-structured mesh. (B-D) Schematic diagram of (B) an oil droplet, (C) a liquid polymer droplet, and (D) a bubble on the laser-structured mesh in a water medium. Water droplet in (A) is at the Wenzel state. The oil droplet, the polymer droplet, and the bubble in (B-D) are at the (underwater) Cassie state

The underwater bubble is repelled by the laser-induced microstructure and maintains a spherical shape to reach minimum free energy. The Cassie wetting state of the underwater bubble on the structured mesh results in the underwater superaerophobicity for the mesh (Figure 2D), so the structured mesh also greatly repel bubbles in water. The laser-induced superhydrophilic microstructures enable the oil droplets, liquid polymer droplets, and bubbles to be at the Cassie state on the stainless steel mesh in water, thereby endowing the mesh with underwater superoleophobicity, superpolymphobicity, and superaerophobicity. If the mesh is not modified by laser processing, it will just show weak oleophobicity, polymphobicity, and aerophobicity in water. The surface wettability can not reach the extreme state for the original mesh.

2.2 | Oil/water separation based on underwater superoleophobicity

The accident of the oil spill and the discharge of industrial oily wastewater frequently occur, which result in economic losses and also seriously pollute the ecological environment.[11–15] The technology for separating oil/water mixtures has become a worldwide research topic to protect the environment. Recently, superhydrophobic or underwater superoleophobic materials have been successfully applied in oil/water separation.[16–22] By taking the advantage of the different interfacial effects of the laser-structured stainless steel mesh to water and oil, the underwater superoleophobic mesh has the ability to achieve oil/water separation (Movie S3, Supporting Information). A simple separation device is designed, as shown in Figure 3A. Many holes with a diameter of ~1.5 mm are previously prepared on the bottle cap of a plastic bottle by mechanically drilling. The laser-structured mesh is used as the separation membrane and is placed inside the bottle cap. Then, the cap is tightened on the plastic bottle whose bottom half is removed. The plastic bottle is placed upside down. Before separation, a small amount of water is first poured into the separating device to pre-wet the structured mesh (Figure 3B). When the mixture of oil (petroleum ether, red color, dyed with oil red O) and water (blue color, dyed with methylene blue) is poured into the separation system (Figure 3C), the water in the mixture can easily penetrate the mesh and drip into the collecting beaker below because the mesh is superhydrophilic. By contrast, the underwater superoleophobicity allows the mesh to repel and intercept the oil phase. The oil in the mixture cannot pass through the mesh and always maintains above the mesh. As a result, the oil/water mixture is successfully separated in a very short time (Figure 3D). Such a separation process is just driven by gravity and can be repeated in many cycles. The separation efficiency can be calculated by $\eta = m_1/m_0$, where m_0 is the mass of the oil in the mixture before separation and m_1 is the mass of the collected oil after separation.[41,42] The separation efficiency is measured to be 98.1%, indicating a

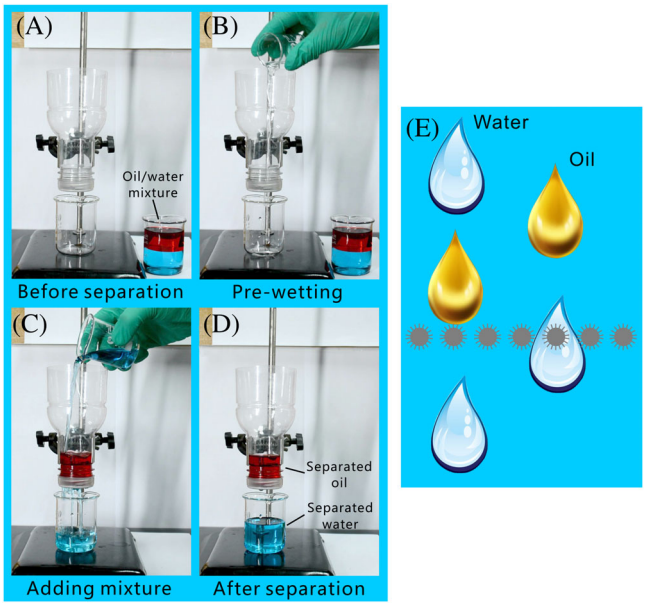

FIGURE 3 Oil/water separation by the laser-structured underwater superoleophobic mesh. A, The designed separation device. B, Prewetting the mesh with water. C, Adding the oil/water mixture into the separation system. D, After separation. E, Mechanism of the oil/water separation based on the underwater superoleophobic mesh. For observing more clearly, oil is dyed by Oil Red O (red color), and water is dyed by methylene blue (blue color)

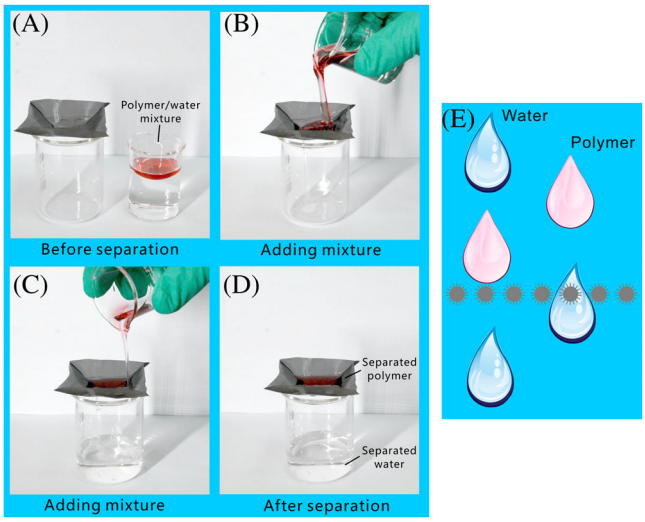

FIGURE 4 Separating liquid polymer from water by the underwater superpolymphobic mesh. A, Before separation. The mesh is pre-wetted with water. (B,C) Pouring the polymer/water mixture onto the structured mesh. D, After separation. E, Mechanism of the polymer/water separation by using the laser-structured underwater superpolymphobic mesh. For observing more clearly, the liquid polymer is dyed by Oil Red O (red color)

perfect performance of the laser-structured stainless steel mesh in oil/water separation. The great oil/water separation ability of the as-prepared mesh is mainly the result of the superhydrophilicity and underwater superoleophobicity of the laser-induced microstructures. The superhydrophilicity allows water to wet and pass through the mesh holes quickly, whereas the underwater superoleophobicity enables the prewetted mesh to repel oils and prevents oil from touching and penetrating the prewetted mesh, as shown in Figure 3E.

2.3 | Polymer/water separation based on underwater superpolymphobicity

Polymers are broadly applied in the chemical industry, energy development, food package, pharmaceuticals, building, lifestyle products, agriculture, etc. With the widespread applications of liquid polymers, the leakage of liquid polymers into the water results in big waste and even various polymer pollutants in water. The traditional treatments for removing polymer pollutants from wastewater can be classified into three representative methods: (i) solidifying and separating from water by coagulation, flocculation, and precipitation, (ii) detoxication treatments such as chemical oxidation and photodegradation, and (iii) adsorption using solid adsorbents like an activated carbon.[43,44] However, the polymer pollutants with high viscosity and low fluidity are easy to adhere to a solid substrate, so they are difficult to be removed from water effectively and on a large scale by using these common methods. Recently, we proposed the concept of "underwater superpolymphobicity" that a surface greatly repels liquid polymers in water.[23–25] The repellence of underwater superpolymphobic materials to liquid polymers provides a possibility to separate polymer from water to alleviate the waste and environmental pollutions caused by liquid polymers.

Similar to the process of oil/water separation, Figure 4A-D and Movie S4 (Supporting information) depict the process of separating the mixture of liquid polymers and water by using the structured mesh as a separation membrane. A piece of the structured mesh is folded into a funnel-like shape. Then, it is pre-wetted by a little water in advance and mounted on a beaker (Figure 4A). After pouring the mixture of liquid polymer (e.g., liquid polydimethylsiloxane (PDMS), red color, dyed with oil red O) and water onto the structured mesh, it is found that only water can quickly permeate through the mesh and drip into the collecting beaker below (Figure 4B). In contrast, the underwater superpolymphobicity of the femtosecond laser-induced microstructures makes the structured mesh intercept the liquid polymer, so the liquid polymer stays on the mesh all the time (Figure 4C). As a result, the mixture of liquid polymer and water is separated and finally

divides into two independent parts: the separated water and the separated polymer (Figure 4D). The schematic of the polymer/water separation is displayed in Figure 4E. The water phase in the mixture can wet and penetrate the structured mesh, driven by superhydrophilicity and gravity force. On the contrary, the prewetted mesh has great ability to repel liquid polymers because of the underwater superpolymphobicity of the laser-induced rough microstructure. Therefore, the polymer phase in the mixture is prevented from passing through the mesh and maintains above the mesh during the whole separation process. It is noticed that there is no liquid polymer remaining in the separated water after the separation treatment. The separation efficiency is calculated by $\eta = m_1/m_0$, where m_1 and m_0 are the mass of the collected polymer after separation and the polymer in the mixture before separation, respectively.[41,42] The laser-induced underwater superpolymphobic mesh has a high separation efficiency of ~98.9% for the polymer/water mixture. The cleaned mesh can be repeatedly used to separate the polymer/water mixtures. Furthermore, such a wettability-based separation method can be extended to various polymer/water mixtures.

The abovementioned polymer/water separation and oil/water separation are different processes although they are based on similar separation mechanism. Entirely different application conditions are required for these two separation systems. The property of high viscosity, low fluidity, and complex composition of liquid polymers increase the difficulty to separate a polymer/water mixture than an oil/water mixture. The separation of liquid polymers from water by using underwater superpolymphobic materials can save polymer resources and prevent polymer based environmental pollution. It should also be noticed that the structured mesh needs to be pre-wetted by water before oil/water separation and polymer/water separation, otherwise both oil (polymer) and water can pass through the metal mesh. The reason is that such a separation is benefited from the underwater superoleophobicity and superpolymphobicity of the laser-structured mesh; that is, the mesh can be wetted by water and only the wetted mesh repel oils and liquid polymers.

2.4 | Bubble/water separation based on underwater superaerophobicity

In some cases, bubbles in liquid can cause some adverse effects.[26,27] For example, the bubbles in a microfluidic system can increase fluid resistance and even block microchannels. In the electrochemical reactions that produce some gases, if a large number of the generated bubbles adhere to the electrode surface, the effective contact between the subsequent electrolyte and the electrode will be hindered, thus greatly reducing the reaction efficiency.[45,46] During the human body transfusion, the bubble in the infusion tube into the blood vessel will cause an embolism, and even endanger the life and health of the patient. A large amount of poisonous sulfide gas and ammonia gas are often dissolved in various industrial wastewater. If the bubbles of these gases can be collected or removed in advance, the pollution degree of the wastewater discharged to the environment can be greatly reduced. Separating tiny bubbles from the liquid is one of the effective ways to solve the abovementioned bubbles-caused problems. An efficient bubble/water separation method will have wide applications in energy utilization, environmental protection, medical and health care, microfluidic chip, chemical manufacturing, agricultural breeding, etc.

The remarkable repellence of the laser-structured mesh to underwater bubbles can be used to separate bubbles from the water. As shown in Figure 5A, the as-prepared underwater superaerophobic mesh is inserted in a water pipe. The mesh is perpendicular to the direction of the water flow. Because the mesh also has superhydrophilicity, so the water flow can easily pass through the mesh and move forward (Figure 5A). If bubbles appear in the water flow, the bubbles will go forward with the water flow. As long as the bubbles arrive at the front side of the mesh, they will be intercepted by the mesh (Figure 5B). All the bubbles are unable to pass through the mesh because of its excellent underwater superaerophobicity (Figure 5C,D). The intercepted bubbles finally merge into a gas space in the front of the mesh and the gas can be easily expelled from the water pipe through a small side hole. As a result, the bubbles are separated from the water flow. The separation efficiency is approximately 100% since no bubbles are detected in the water flow after separation. Figure 5E shows the separation mechanism based on the superhydrophilic and underwater superaerophobic mesh. The superhydrophilicity allows water flow to wet and across the mesh, ensuring the normal circulation of water. On the contrary, the structured mesh shows remarkable repellence to bubbles in water because of the underwater superaerophobicity. The bubbles in water flow is intercepted by the mesh and are unable to pass through the mesh. The smaller the holes of the structured mesh, the smaller the bubble can be intercepted. So, almost all bubbles in water flow can be removed by the underwater superaerophobic porous membrane with extremely small pores. On the other hand, a small side hole or a gas channel can be used to timely expel the intercepted bubble/gas from the water pipe, to avoid the gas accumulation in practical applications.

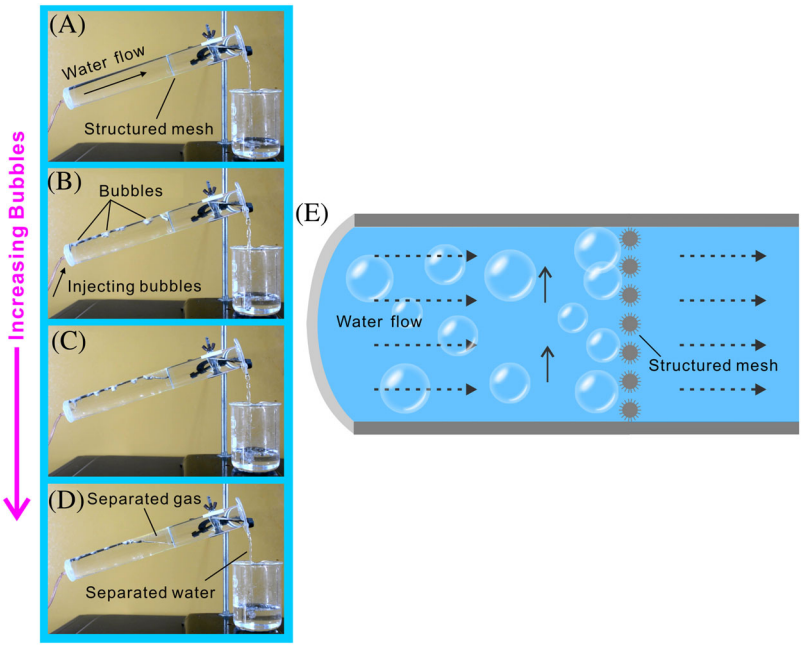

FIGURE 5 Separating bubbles from water flow by the underwater superaerophobic mesh. A, Water freely passing through the mesh inserted in a water pipe. (B-D) Intercepting function of the underwater superaerophobic mesh to the bubbles in the water flow. E, Mechanism of the bubble/water separation by the underwater superaerophobic mesh

3 | CONCLUSIONS

In conclusion, we extend the method of superwettability-based oil/water separation to treat the mixtures of liquid polymers and water and separate bubbles from water. Superwetting micro/nanoscale structures are prepared on the surface of a stainless steel mesh by femtosecond laser treatment. The rough surface microstructures make the mesh superhydrophilic as water can fully wet the mesh. A small oil droplet, polymer droplet, and bubble on the structured mesh have a CA of 154.8° ± 1.2°, 156.3° ± 0.7°, and 153.7° ± 1.3° in water, respectively. As long as the mesh is slightly tilted, the underwater oil droplet, polymer droplet, and bubble will roll away easily. The results demonstrate that the formation of the laser-induced microstructures endows the mesh with underwater superoleophobicity, superpolymphobicity, and superaerophobicity. The resultant mesh exhibits strong repellence to oils, liquid polymers, and bubbles in the water. Based on the underwater superoleophobicity, superpolymphobicity, and superaerophobicity, the oil/water mixture, the polymer/water mixture, and the bubble/water mixture are separated by using the structured mesh. Superhydrophilicity allows water to penetrate the structured mesh, whereas the oils, the liquid polymers, and the bubbles in water are intercepted by the mesh due to the remarkable oil/polymer/bubble repellence of the laser-induced microstructures. As a result, the oil, the liquid polymer, and the bubble are successfully separated from water with a very high separation efficiency by using the as-prepared superwetting mesh. In addition to oil/water separation, polymer/water separation, and bubble/water separation, the reported separation strategy based on superwettability can potentially be applied in various kinds of liquid-liquid mixtures and liquid-gas mixtures. We believe that the diversified wettability-based separation processes will have wide applications in environmental protection, energy utilization, industrial manufacture, agricultural production, and so on.

4 | EXPERIMENTAL SECTION

4.1 | Femtosecond laser processing

Rough microstructures were prepared on the wire surface of a stainless steel mesh (500 mesh size, with a pore diameter of ~32.3 μm) by femtosecond laser ablation. The mesh was mounted on a moveable stage. The 50 fs laser beam (center wavelength = 800 nm; repetition rate = 1 kHz) from a regenerative amplified Ti:sapphire system (Coherent Libra-usp-he) was focused onto the mesh surface through a plano-convex lens (focal length = 200 mm). During the line-by-line laser scanning process, the scanning speed was 2 mm s^{-1} and the scanning space was 50 μm at the laser power of 300 mW. After laser treatment, the meshes were carefully cleaned.

4.2 | Oil/water separation

A simple oil/water separation device was prepared by using the laser-structured mesh as the separation membrane. The structured mesh was placed inside the bottle cap of a plastic bottle, as shown in Figure 3A. The bottom

half of the plastic bottle was removed and many large holes (diameter of ~1.5 mm) are previously drilled on the bottle cap. The plastic bottle is placed upside down. The separation membrane was prewetted by water before separation. Then, the ~ 60 mL mixture of oil (petroleum ether) and water with the volume rate of ~1:1 was feed into the separation system. For clear observation, the used oil was dyed by Oil Red O and the water was dyed by methylene blue.

4.3 | Polymer/water separation

The separation process for polymer/water mixture is similar to that of the oil/water separation. A piece of the structured mesh was folded into a funnel-like shape, pre-wetted by water, and then placed above a beaker, as shown in Figure 4A. The separation process started with pouring the ~25 mL mixture of liquid polymer (uncured PDMS liquid) and water (volume ratio of polymer to water = ~1: 4) onto the structured mesh. For clear observation, the liquid polymer was dyed red with Oil Red O and showed a red color.

4.4 | Bubble/water separation

As shown in Figure 5A, the laser-structured mesh was inserted in a water pipe, placing perpendicular to the direction of the water flow. With the water flowing forward, small bubbles were continually introduced in the water flow through an injection syringe. The flow rate of the incoming gas was about 1.2 mL s^{-1}. The bubbles gone with the water flow and arrived at the front side of the inserted mesh. It was demonstrated that all of the bubbles were intercepted by the laser-structured mesh.

4.5 | Characterization

The surface morphology of the mesh was observed through a FlexSEM-1000 scanning electron microscope (Hitachi, Japan). The wettabilities of a water droplet, oil droplet, liquid polymer droplet, and gas bubble on the mesh surface were measured by a JC2000D contact-angle measurement (Powereach, China). The distilled water, 1,2-Dichloroethane, uncured polydimethylsiloxane (PDMS) (DC-184, Dow Corning Corporation), and air were adopted as the main tested water, oil, liquid polymer, and bubble, respectively. The processes of oil/water separation, polymer/water separation, and bubble/water separation were captured by a D7100 camera (Nikon, Japan). For the oil/water separation and the polymer/water separation, the separation efficiency was calculated by $\eta = m_1/m_0$, where m_1 and m_0 are the mass of the collected oil/polymer and the oil/polymer before separation, respectively.[41,42] The separation efficiency of the bubble/water mixture was obtained by analyzing the bubble number in water flow before and after separation; that is, it can be calculated by $\eta = (n_0 - n_1)/n_0$, where n_0 is the number of bubbles that introduced into the water flow and n_1 is the number of bubbles in the separated water flow.

ACKNOWLEDGMENTS

(This work is supported by the National Key Research and Development Program of China (2017YFB1104700), the National Science Foundation of China (61805192 and 61875158), the International Joint Research Laboratory for Micro/Nano Manufacturing and Measurement Technologies, and the Fundamental Research Funds for the Central Universities.)

DATA AVAILABILITY STATEMENT

Data sharing is not applicable to this article as no new data were created or analyzed in this study.

ORCID

Feng Chen https://orcid.org/0000-0002-7031-7404

REFERENCES

1. J. Li, R. J. Kuppler, H.-C. Zhou, *Chem. Soc. Rev.* **2009**, *38*, 1477.
2. A. Hyman, C. A. Weber, F. Juelicher, *Annu. Rev. Cell Dve. Bi.* **2014**, *30*, 39.
3. J.-R. Li, J. Sculley, H.-C. Zhou, *Chem. Rev.* **2012**, *112*, 869.
4. S. Qiu, M. Xue, G. Zhu, *Chem. Soc. Rev.* **2014**, *43*, 6116.
5. M. Hu, B. Mi, *Environ. Sci. Technol.* **2013**, *47*, 3715.
6. J. Zhang, Z. Li, K. Zhan, R. Sun, Z. Sheng, M. Wang, S. Wang, X. Hou, *Electrophoresis* **2019**, *40*, 2029.
7. W. Lv, Z. Sheng, Y. Zhu, J. Liu, Y. Lei, R. Zhang, X. Chen, X. Hou, *Microsyst. Microeng.* **2020**, *6*, 43.
8. X. Hou, *Adv. Mater.* **2016**, *28*, 7049.
9. X. Hou, *Natl. Sci. Rev.* **2020**, *7*, 9.
10. Z. Sheng, H. Wang, Y. Tian, M. Wang, L. Huang, L. Min, H. Meng, S. Chen, L. Jiang, X. Hou, *Sci. Adv*. **2018**, *4*, eaao6724.
11. B. Wang, W. Liang, Z. Guo, W. Liu, *Chem. Soc. Rev.* **2015**, *44*, 336.
12. J. Yong, J. Huo, F. Chen, Q. Yang, X. Hou, *Phys. Chem. Chem. Phys.* **2018**, *20*, 25140.
13. Z. Chu, Y. Feng, S. Seeger, *Angew. Chem. Int. Ed.* **2015**, *54*, 2328.
14. J. Yong, Q. Yang, C. Guo, F. Chen, X. Hou, *RSC Adv.* **2019**, *9*, 12470.
15. R. K. Gupta, G. J. Dunderdale, M. W. England, A. Hozumi, *J. Mater. Chem. A* **2017**, *5*, 16025.
16. Q. Zhu, Q. Pan, F. Liu, *J. Phys. Chem. C* **2011**, *115*, 17464.
17. J. L. Yong, Y. Fang, F. Chen, J. Huo, Q. Yang, H. Bian, G. Du, X. Hou, *Appl. Surf. Sci.* **2016**, *389*, 1148.
18. Y.-Q. Liu, Y.-L. Zhang, X.-Y. Fu, H.-B. Sun, *ACS Appl. Mater. Interfaces* **2015**, *7*, 20930.
19. J. L. Yong, F. Chen, Q. Yang, G. Du, C. Shan, J. Huo, Y. Fang, X. Hou, *Adv. Mater. Interfaces* **2016**, *3*, 1500650.

20. G. Li, H. Fan, F. Ren, C. Zhou, Z. Zhang, B. Xu, S. Wu, Y. Hu, W. Zhu, J. Li, Y. Zeng, X. Li, J. Chu, D. Wu, *J. Mater. Chem. A* **2016**, *4*, 18832.
21. L. Feng, Z. Zhang, Z. Mai, Y. Ma, B. Liu, L. Jiang, D. Zhu, *Angew. Chem. Int. Ed.* **2004**, *43*, 201.
22. Z. Xue, S. Wang, L. Lin, L. Chen, M. Liu, L. Feng, L. Jiang, *Adv. Mater.* **2011**, *23*, 4270.
23. J. Yong, S. C. Singh, Z. Zhan, E. Mohamed, F. Chen, C. Guo, *ACS Appl. Nano Mater.* **2019**, *2*, 7362.
24. J. Yong, Z. Zhan, S. C. Singh, F. Chen, C. Guo, *Langmuir* **2019**, *35*, 9318.
25. J. L. Yong, Z. Zhan, S. C. Singh, F. Chen, C. Guo, *ACS Appl. Polym. Mater.* **2019**, *1*, 2819.
26. C. Yu, P. Zhang, J. Wang, L. Jiang, *Adv. Mater.* **2017**, *29*, 1703053.
27. J. E. George, S. Chidangil, S. D. George, *Adv. Mater. Interfaces* **2017**, *4*, 1601088.
28. J. Yong, F. Chen, Y. Fang, J. Huo, Q. Yang, J. Zhang, H. Bian, X. Hou, *ACS Appl. Mater. Interfaces* **2017**, *9*, 39863.
29. Y. Jiao, C. Li, X. Lv, Y. Zhang, S. Wu, C. Chen, Y. Hu, J. Li, D. Wu, J. Chu, *J. Mater. Chem. A* **2018**, *6*, 20878.
30. Y. Tian, B. Su, L. Jiang, *Adv. Mater.* **2014**, *26*, 6872.
31. L. Wen, Y. Tian, L. Jiang, *Angew. Chem. Int. Ed.* **2015**, *54*, 3387.
32. J. Yong, F. Chen, M. Li, Q. Yang, Y. Fang, J. Huo, X. Hou, *J. Mater. Chem. A* **2017**, *5*, 25249.
33. B. Su, Y. Tian, L. Jiang, *J. Am. Chem. Soc.* **2016**, *138*, 1727.
34. J. Yong, Q. Yang, X. Hou, F. Chen, *Front. Chem.* **2020**, *8*, 808.
35. J. Yong, F. Chen, Q. Yang, J. Huo, X. Hou, *Chem. Soc. Rev.* **2017**, *46*, 4168.
36. J. Yong, F. Chen, Q. Yang, Z. Jiang, X. Hou, *Adv. Mater. Interfaces* **2018**, *5*, 1701370.
37. T. Jiang, Z. Guo, W. Liu, *J. Mater. Chem. A* **2015**, *3*, 1811.
38. B. Wu, M. Zhou, J. Li, X. Ye, G. Li, L. Cai, *Appl. Surf. Sci.* **2009**, *256*, 61.
39. S. Wang, L. Jiang, *Adv. Mater.* **2007**, *19*, 3423.
40. M. Liu, S. Wang, L. Jiang, *Nat. Rev. Mater.* **2017**, *2*, 17036.
41. J. Li, D. Li, Y. Yang, J. Li, F. Zha, Z. Lei, *Green Chem.* **2016**, *18*, 541.
42. J. Yong, Q. Yang, X. Hou, F. Chen, *Front. Phys.* **2020**, *8*, 305.
43. S. Mizuno, T.A. Asoh, Y. Takashima, A. Harada, H. Uyama, *Polym. Degrad. Stabil.* **2019**, *160*, 136.
44. M.-L. Liu, L. Li, Y.-X. Sun, Z.-J. Fu, X.-L. Cao, S.-P. Sun, *J. Membrane Sci.* **2021**, *617*, 118644.
45. Z. Lu, W. Zhu, X. Yu, H. Zhang, Y. Li, X. Sun, X. Wang, H. Wang, J. Wang, J. Luo, X. Lei, L. Jiang, *Adv. Mater.* **2014**, *26*, 2683.
46. Z. Lu, M. Sun, T. Xu, Y. Li, W. Xu, Z. Chang, Y. Ding, X. Sun, L. Jiang, *Adv. Mater.* **2015**, *27*, 2361.

SUPPORTING INFORMATION

Additional supporting information may be found online in the Supporting Information section at the end of the article.

How to cite this article: Yong J, Yang Q, Huo J, Hou X, Chen F. Superwettability-based separation: From oil/water separation to polymer/water separation and bubble/water separation. *Nano Select*. **2021**;*2*:1580–1588.
https://doi.org/10.1002/nano.202000246